

Rheology of distorted nematic liquid crystals

D. MARENUZZO¹, E. ORLANDINI² AND J.M. YEOMANS¹

¹*Department of Physics, Theoretical Physics, 1 Keble Road, Oxford OX1 3NP, England*

²*INFN, Dipartimento di Fisica, Universita' di Padova, Via Marzolo 8, 35131 Padova, Italy*

PACS. 83.80.Xz – Liquid crystals: nematic, cholesteric, smectic, discotic, etc..

PACS. 47.50+d – Non-Newtonian fluid flows.

Abstract. – We use lattice Boltzmann simulations of the Beris–Edwards formulation of nematodynamics to probe the response of a nematic liquid crystal with conflicting anchoring at the boundaries under shear and Poiseuille flow. The geometry we focus on is that of the hybrid aligned nematic (HAN) cell, common in devices. In the nematic phase, backflow effects resulting from the elastic distortion in the director field render the velocity profile strongly non-Newtonian and asymmetric. As the transition to the isotropic phase is approached, these effects become progressively weaker. If the fluid is heated just above the transition point, however, another asymmetry appears, in the dynamics of shear band formation.

Introduction. – Non-Newtonian behaviour in complex fluids such as liquid crystals arises because of the coupling between the molecular ordering, described by the director field, and the flow field. Liquid crystal molecules can be aligned by a shear or rotational flow [1,2] and, conversely, movement of the molecules can induce a velocity field, the so-called back-flow. This coupling results in flow-induced instabilities, such as tumbling under shear, where the director field rotates in a time-dependent steady state. An even more striking example is the banded texture that is predicted upon shearing a nematic liquid crystal in the vicinity of the nematic-isotropic transition [3,4]. Moreover, in twisted nematic devices the phenomenon of optical bounce, a transient rotation of the director field in the center of the cell in the wrong direction upon switching, has been well studied and is understood to be due solely to back-flow [5]. More recently, there have been detailed measurements of back-flow effects on another commonly used cell, namely the hybrid aligned nematic (HAN) cell [6].

As a result of extensive theoretical, numerical and experimental investigations the behaviour of nematic liquid crystals in shear and Poiseuille flow fields is well documented [7,8,9,10,11,12,13]. However as far as we are aware results are limited to the cases where at *all* the boundaries of the containing cell the alignment of the director field is either free, homogeneous (parallel to the surface) or homeotropic (perpendicular to the surface).

This is perhaps surprising, given the widespread use in displays of nematics with elastic distortions [14,15]. An elastic deformation appears in the unsheared state of a nematic liquid crystal when a rotation is imposed on the director field by conflicting anchoring at opposite boundaries.

In trying to minimize its elastic free energy the system adopts a uniform deformation across the sample. One might expect the interplay between such a distorted director field and the flow field to lead to unexpected non-Newtonian behaviour. Therefore the aim of this paper is to present results for the behaviour of distorted liquid crystalline systems under shear and Poiseuille flow.

We find that the imposed anchoring can strongly affect both the transient and the steady state properties of the flow. Focusing on a cell with mixed homeotropic and homogeneous anchoring, corresponding to the geometry of the HAN cell, we show that at low temperatures, deep in the nematic phase, the elastic distortion strongly affects the velocity profile and introduces an asymmetry. As the temperature increases, or equivalently as the parameters change so as to render director re-orientation due to the external flow less costly, the asymmetry is progressively reduced. As a result the liquid crystal rheology can, to a fair approximation, be described by that of a Newtonian fluid. Near the isotropic–nematic transition the fluid again exhibits its non-Newtonian nature and another asymmetry develops, this time in the way banded textures develop in the system.

Equations of motion. – We follow the Beris–Edwards formulation of nematodynamics [2] and write the hydrodynamic continuum equations of motion in terms of a tensor order parameter \mathbf{Q} whose largest eigenvalue, $\frac{2}{3}q$, $0 < q < 1$, describes the magnitude of the order.

The equilibrium properties of the liquid crystal are described by the following Landau-de Gennes free energy density

$$f = \frac{A_0}{2} \left(1 - \frac{\gamma}{3}\right) Q_{\alpha\beta}^2 - \frac{A_0\gamma}{3} Q_{\alpha\beta} Q_{\beta\gamma} Q_{\gamma\alpha} + \frac{A_0\gamma}{4} (Q_{\alpha\beta}^2)^2 + \frac{K}{2} (\partial_\alpha Q_{\beta\gamma})^2, \quad (1)$$

where A_0 is a constant and Greek indices label the Cartesian components of \mathbf{Q} . Eq. 1 comprises a bulk contribution which describes a first order transition from the isotropic to the uniaxial nematic phase at $\gamma = 2.7$, together with an elastic contribution – penalizing distortions – depending on the elastic constant K .

The anchoring of the director field on the boundary surfaces (Fig. 1) to a chosen director \hat{n}^0 is ensured by adding the surface term

$$f_s = \frac{1}{2} W_0 (Q_{\alpha\beta} - Q_{\alpha\beta}^0)^2, \quad Q_{\alpha\beta}^0 = S_0 (n_\alpha^0 n_\beta^0 - \delta_{\alpha\beta}/3). \quad (2)$$

The parameter W_0 controls the strength of the anchoring, while S_0 determines the degree of surface order [16, 17].

The equation of motion for the nematic order parameter is [2]

$$(\partial_t + \vec{u} \cdot \nabla) \mathbf{Q} - \mathbf{S}(\mathbf{W}, \mathbf{Q}) = \Gamma \mathbf{H} \quad (3)$$

where Γ is a collective rotational diffusion constant. The term on the left-hand side is:

$$\mathbf{S}(\mathbf{W}, \mathbf{Q}) = (\xi \mathbf{D} + \mathbf{\Omega})(\mathbf{Q} + \mathbf{I}/3) + (\mathbf{Q} + \mathbf{I}/3)(\xi \mathbf{D} - \mathbf{\Omega}) - 2\xi(\mathbf{Q} + \mathbf{I}/3)\text{Tr}(\mathbf{Q}\mathbf{W}) \quad (4)$$

where $\mathbf{D} = (\mathbf{W} + \mathbf{W}^T)/2$ and $\mathbf{\Omega} = (\mathbf{W} - \mathbf{W}^T)/2$ are the symmetric part and the anti-symmetric part respectively of the velocity gradient tensor $W_{\alpha\beta} = \partial_\beta u_\alpha$. The constant ξ depends on the molecular details of a given liquid crystal. The molecular field \mathbf{H} of Eq. (3) describes the relaxation of the order parameter towards the minimum of the free energy [2].

The fluid velocity, \vec{u} , obeys the continuity equation and the Navier-Stokes equation,

$$\rho(\partial_t + u_\beta \partial_\beta) u_\alpha = \partial_\beta \tau_{\alpha\beta} + \partial_\beta \sigma_{\alpha\beta} + \eta \partial_\beta ((1 - 3\partial_\rho P_0) \partial_\gamma u_\gamma \delta_{\alpha\beta} + \partial_\alpha u_\beta + \partial_\beta u_\alpha), \quad (5)$$

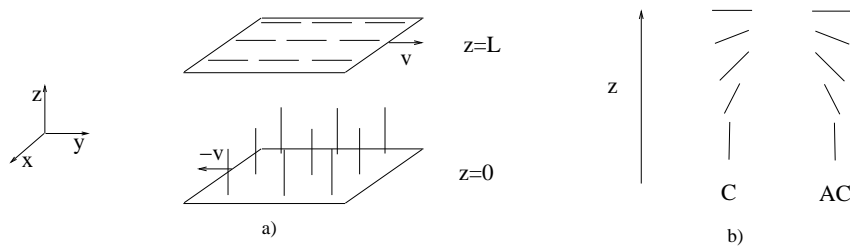


Fig. 1 – a) Geometry used for the calculations described in the text. The liquid crystal is sandwiched between two infinite plates, parallel to the xy plane, lying at $z = 0$ and $z = L$. The anchoring is homeotropic on the bottom plate and homogeneous, along the flow direction, on the top plate. The figure refers to the case of an imposed shear flow. b) Sketch of the director field profile along the \hat{z} direction with no applied flow. The director can adopt the two degenerate configurations shown which we label as a clockwise (profile C) or anti-clockwise (AC) rotation. Unless otherwise stated we focus here on the case in which the director adopts the C configuration in the absence of flow.

where ρ is the fluid density and η is an isotropic viscosity. The quantities $\sigma_{\alpha\beta}$ and $\tau_{\alpha\beta}$ are the symmetric and antisymmetric part of the stress tensor respectively.

The equations for order parameter field Eq. (3) and flow field Eq. (5) are coupled. The velocity field and its derivatives appear in the equation of motion for the order parameter. Conversely, the order parameter field affects the dynamics of the flow field through the stress tensor which appears in the Navier-Stokes equation (5) and depends on \mathbf{Q} and \mathbf{H} . This back-action of the order parameter field on the flow field is commonly termed backflow. To solve these equations we use a lattice Boltzmann algorithm, the details of which (for the two-dimensional case) have been given in Ref. [18] and further discussed in Ref. [19].

Poiseuille flow in the nematic phase. – We consider a liquid crystal confined between two plates which lie parallel to the x - y plane at $z = 0$ and $z = L$. A rotation of $\pi/2$ about the x -axis, corresponding to a splay/bend deformation, is imposed on the director field by fixing the anchoring to be homogeneous along \hat{y} at $z = L$ and homeotropic (i.e. along \hat{z}) at $z = 0$ as shown in Figure 1. The angle the director makes with the z axis varies linearly between the plates. This geometry is the one defining the HAN cell [1, 6].

We first report the results obtained when the system is subject to a Poiseuille flow along \hat{y} . Figure 2a shows plots of the velocity field across the system and the comparison to the parabolic profile, expected for a Newtonian fluid, obtained if backflow is neglected. (Backflow was ‘turned off’ in the numerical simulations by imposing $\sigma_{\alpha\beta} = -P_0\delta_{\alpha\beta}$, with P_0 a constant, and $\tau_{\alpha\beta} = 0$ in Eq. (5).) The difference between the two cases is remarkable. Back-flow renders the rheology of the liquid crystal markedly non-Newtonian. First, the typical velocity in the system is more than a factor of two smaller. Second, it is asymmetric.

It is possible to explain the asymmetry of the velocity in an intuitive way. The conflicting anchoring conditions of the HAN cell geometry yield a director profile in which a wide range of orientations coexist simultaneously in the sample in the absence of external perturbation (this remains true when the pressure difference applied to impose the flow is low). As these orientations couple differently to the imposed flow, via the back-flow, the steady state displays an asymmetry.

Figure 2b shows how the deviation from the parabolic velocity profile varies with temperature. (We consider γ as an effective temperature as it controls the isotropic-nematic transition.) It can

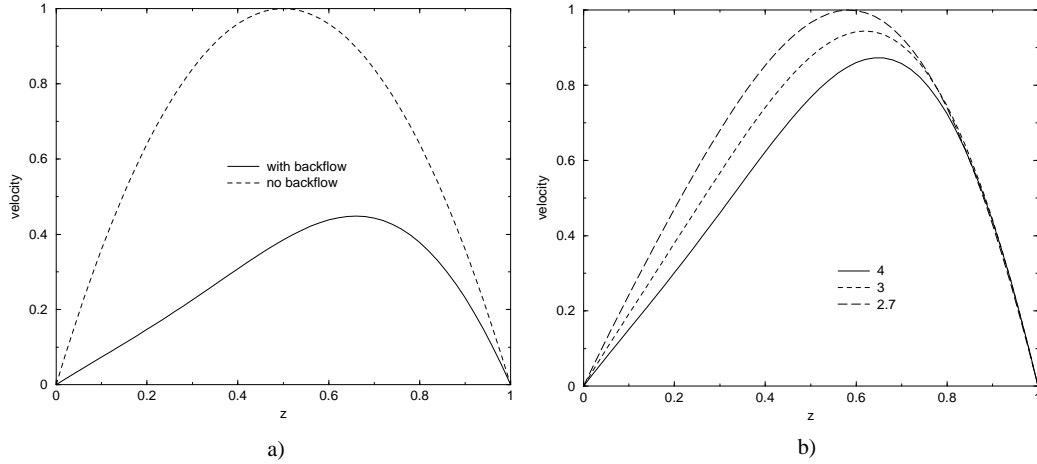


Fig. 2 – Velocity profiles under Poiseuille flow. (a) $\gamma = 5$ for a channel of width $1 \mu\text{m}$. The velocity has been divided by $7 \cdot 10^{-5} \frac{A_0 L}{\Gamma}$ to make it dimensionless and with unit maximum. (b) $\gamma = 4, 3, 2.7$ for a channel of width $1 \mu\text{m}$. The velocity has been divided by $3.8 \cdot 10^{-5} \frac{A_0 L}{\Gamma}$.

be seen that as the temperature approaches that of the isotropic-nematic transition and thus the magnitude of the order decreases, the velocity profile approaches that of a standard Newtonian fluid. Non-Newtonian effects also decrease when the system size is increased because director reorientation is easier and when the flow rate is increased because the relative contribution of backflow is less.

Shear flow in the nematic phase. – Let us now discuss the behaviour of the same HAN cell under a constant applied shear. Consider first an imposed shear along \hat{y} (Fig. 1). In a Newtonian fluid this would give a linear velocity profile. However now, in steady state flow conditions, the strain rate is not constant, and the velocity field deviates from linear because of the different coupling of the flow to the director field as z varies.

Fig. 3 shows how the scaled velocity profile in the channel depends on the system parameters. When director field reorientation is more difficult due to a narrow width (Fig. 3a), to a low temperature (data not shown) or to low shear rates (Fig. 3b) the asymmetry is more pronounced. This effect is qualitatively similar to the one observed with Poiseuille flow.

Consider the case of increasing shear rate (Fig. 3b) when an interesting structure appears in the director field as the fluid velocity increases. The cell tends to spontaneously separate into two distinct regions characterised by different director configurations with a rather sharp crossover between them. In the top portion of the cell, the strain rate is higher and the fluid is well aligned with the flow and resembles a standard nematic. All the elastic distortion is confined to the bottom portion of the cell where the strain rate gradually decreases. The boundary between the two regions moves nearer to the homeotropic plate as the shear rate increases. This is an example of shear-induced patterning of the director configuration across the cell, a phenomenon which we will encounter again below, when we discuss banding dynamics near the isotropic-nematic transition.

A few remarks are now in order: first, it is to be noted that the two configurations in which the director performs a clockwise or anti-clockwise rotation around the \hat{x} direction (configurations

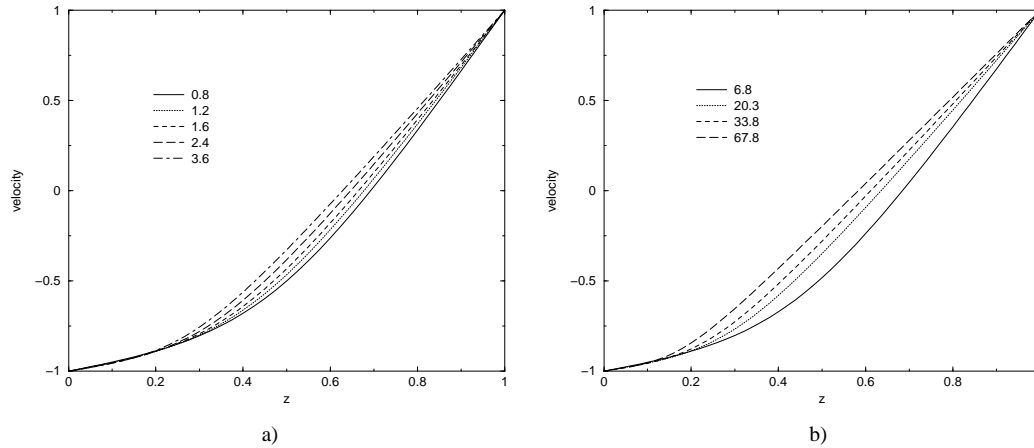


Fig. 3 – Velocity profiles across the cell under shear flow for different values of the model parameters. In the plots z is scaled by the system dimension and the velocity is scaled by the maximum velocity in the system, attained at $z = L$. The elastic constant $K = 11.7 \text{ pN}$ for all plots. (a) Velocity profiles for different cell widths L (in micrometers). The shearing velocity is constant (0.7 mm s^{-1}), and $\gamma = 5$ for these plots. (b) Velocity profiles for a cell of width $1 \mu\text{m}$, with $\gamma = 5$ and variable shearing velocities (in dimensionless units, scaled by $10^5 \frac{\Delta\eta L}{\eta}$).

C and AC in Fig.1), which are equally probable in the absence of flow, couple differently to the imposed flow. The results we have just shown refer to the case of a clockwise rotation. If the starting configuration is that labelled AC in Fig. 1, the details of the flow change. In a region which lies at the bottom of the cell and which increases in size with increasing shear, the director field closely resembles that of a smaller cell with homeotropic anchoring on both plates which is subjected to a shear flow.

Second, the behaviour of a nematic liquid crystal in an imposed flow can be either flow aligning or flow tumbling [7]. In the Beris–Edwards model, the behaviour depends on the magnitude of the order and on the parameter ξ [2, 18]. We chose $\xi = 0.85$ so that the liquid crystal is flow aligning in the whole temperature (γ) regime considered. Flow tumbling materials will be considered elsewhere.

Third, we have so far considered the case in which the director field is initially in the flow plane. If the system is sheared along the \hat{x} direction instead, a small secondary flow develops along \hat{y} .

Shear banding near the nematic–isotropic transition. – When a nematic is sheared in the vicinity of the isotropic–nematic boundary (just above the transition temperature) shear bands can form. These are coexisting states, one nematic, one paranematic, with an interface between them which normally lines up along the flow direction. The amount of each coexisting phase depends on the shear rate and the free energies of the competing phases [3] in a way that is not yet fully understood.

When free (i.e. unconstrained) boundary conditions are considered [3], two ordered bands, in which the fluid is locally in a nematic state, can form at the surface of the cell, because of the favourable coupling of an ordered phase to the higher strain rates present near the moving surfaces. These grow symmetrically until they reach a steady state width.

Here we consider the formation of the shear bands in a HAN cell geometry (Figure 1) and show

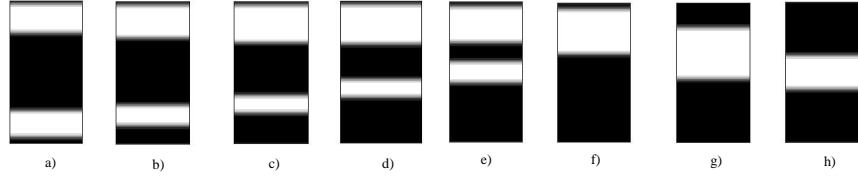


Fig. 4 – Pictures of the formation of shear bands when the boundaries are anchored as described in the text. In this calculation we put the anchoring strength $S_0 = 0.08$ and $\gamma = 2.65$, while the dimensionless ratio $\frac{\Gamma v}{A_0 L} = 7.35 \cdot 10^{-4}$. The plots show the magnitude of the order parameter. Black regions correspond to low order (the system is locally isotropic with q very small) and white regions to high order (the system is locally nematic with $q \sim 0.3$). The graphs correspond to times (a) 0.9 ms, (b) 49.5 ms, (c) 119.7 ms, (d) 270 ms, (e) 711 ms, (f) 855 ms, (g) 911.7 ms, (h) 5.4 s.

that the conflicting boundary conditions introduce an asymmetry into the kinetic pathway by which the bands form. We work at $\gamma = 2.65$ and surface order S_0 between 0.05 and 0.15 so that the fluid is in the isotropic phase, and apply a shear of a few mm s^{-1} (Fig. 4). Because S_0 and W_0 are both non-zero, two thin layers of paranematic order, of thickness a few tens of nm, appear near the boundaries even in the unperturbed state [16,17].

The dynamical evolution of the liquid crystal once shear is applied, in the case of conflicting anchoring at the boundaries, is shown in Fig. 4. First, two bands form at the edges of the cell (as is the case for free boundaries). This is because, as in realistic situations, there is initially a transient large strain rate at the boundaries as it takes time for the shear perturbation to reach the bulk. Quite rapidly, however (after a few ms according to our simulations), the band near the homeotropic surface becomes unstable because the surface anchoring conflicts with the flow alignment angle favoured by the presence of the shear. Thus, the band quickly unbinds from the surface and becomes thinner. It moves across the system to join the band forming at the other surface. This is advantageous because it minimizes the number of interfaces.

At later times, the final steady state reached in the simulations depends on the degree and direction of surface ordering in the top plate. For the case displayed in Fig. 4 ($S_0 = 0.08$ and homogeneous anchoring along the flow direction), the wider band finally unbinds from the top surface and eventually comes to rest in the centre of the system. When the degree of surface ordering is weaker, the stable steady state corresponds to the band remaining at the top of the sample. Mapping the simulation parameters onto physical parameters we estimate that the evolution of the bands takes a few seconds, in a cell of width $\sim \mu\text{m}$, a time scale easily amenable to experiments.

Discussion. – In conclusion, we have studied the response of a nematic liquid crystal with conflicting anchoring at the boundaries, and hence an imposed director distortion, under shear and Poiseuille flow. Specifically, we focussed on the geometry of the hybrid aligned nematic cell and found that when the system is nematic and the strain rate is low, the imposed distortion has a strong effect on the velocity profile via backflow. As a result the fluid behaves in a markedly non-Newtonian manner.

For Poiseuille flow, the effect is particularly visible. The velocity profile becomes strongly asymmetric and the flow rate is strongly suppressed. Under shear, as the shear rate increases, the velocity profile forms two distinct regions with different typical strain rates. One of these regions, which contains virtually all the director deformation, is increasingly confined near one of the boundaries of the cell.

As the degree of order in the sample decreases, due for example to an increase of temperature towards the transition temperature to the isotropic phase, the strain rates across the system become more symmetric and the fluid rheology resembles that of a Newtonian fluid. However, just above the transition temperature, we again observe non-Newtonian behaviour, namely shear banding. The conflicting surface-induced ordering affects the way in which the bands form, introducing a dynamical asymmetry.

A lattice Boltzmann solution of the Beris–Edwards equations proved very powerful for this study. It allowed us to consider fully the effects of temperature, backflow, conflicting anchoring and different degrees of order within the cell on the liquid crystal rheology.

There are several directions in which this work could be pursued. First, one can extend the present treatment to flow tumbling materials and to other cells with elastic distortions, for example the twisted nematic cell, a basic display device. Second, it would be very interesting to study flow in the cells with more complicated boundary conditions which are increasingly being fabricated by modern lithographic techniques. Third, we should like to compare the present picture to the one arising from rheological studies in which distortions are not imposed but are natural, as is the case for example in cholesteric liquid crystals.

Finally, we note that the phenomenology described here is robust over a wide range of parameters in our calculations, and occurs on physically accessible length and time scales. The results can be tested experimentally with technology currently available.

Acknowledgements: We thank C. Denniston for useful and important discussions.

REFERENCES

- [1] P. G. de Gennes and J. Prost, *The Physics of Liquid Crystals, 2nd Ed.*, Clarendon Press, Oxford (1993); S. Chandrasekhar, *Liquid Crystals*, Cambridge University Press, (1980).
- [2] A. N. Beris, B. J. Edwards, *Thermodynamics of Flowing Systems*, Oxford University Press, Oxford (1994).
- [3] P. D. Olmsted, C. Y. D. Lu, *Phys. Rev. E* **60**, 4397 (1999); C. Y. D. Lu, P. D. Olmsted, R. C. Ball, *Phys. Rev. Lett.* **84**, 642 (2000).
- [4] X. F. Yuan, L. Jupp, *Europhys. Lett.* **60**, 691 (2002).
- [5] N. J. Smith, M. D. Tillin, J. R. Sambles, *Phys. Rev. Lett.* **88**, 088301 (2002).
- [6] S. A. Jewell, J. R. Sambles, *J. Appl. Phys.* **92**, 19 (2002).
- [7] A. D. Rey, M. D. Denn, *Annu. Rev. Fluid Mech.* **34**, 233 (2002).
- [8] W. H. Han, A. D. Rey, *Phys. Rev. E* **49**, 597 (1994).
- [9] P. Toth, A. P. Krekhov, L. Kramer, J. Peinke, *Europhys. Lett.* **51**, 48 (2000).
- [10] P. Pieranski, E. Guyon, *Commun. Phys.* **1**, 45 (1976).
- [11] E. Vicente Alonso, A. A. Wheeler, T. J. Sluckin, *Proc. R. Soc. Lond. A* **459**, 195 (2003).
- [12] M. Luskin, T. W. Pan, *J. Non-Newton. Fluid Mech.* **42**, 369 (1992).
- [13] I. Zuniga, F. M. Leslie, *Europhys. Lett.* **9**, 689 (1989).
- [14] E. P. Raynes, C. V. Brown, J. F. Stromer, *Appl. Phys. Lett.* **82**, 13 (2003).
- [15] J. Chen et al., *J. Appl. Phys.* **80**, 1985 (1996).
- [16] P. Galatola, J. B. Fournier, *Phys. Rev. Lett.* **86**, 3915 (2001).
- [17] M. Nobili, G. Durand, *Phys. Rev. A* **46**, R6174 (1992).
- [18] C. Denniston, E. Orlandini, J. M. Yeomans, *Europhys. Lett.* **52**, 481 (2000).
- [19] C. Denniston, E. Orlandini, J. M. Yeomans, *Phys. Rev. E* **63**, 056702 (2001); *Phys. Rev. E* **64**, 021701 (2001); *Comp. Theor. Polym. S.* **11**, 389 (2001).